The residual stress characteristics and mechanical behavior of shot peened fiber metal laminates based on the aluminium-lithium alloy

Li, Huaguan; Wang, Hao; Alderliesten, René; Xiang, Junxian; Lin, Yanyan; Xu, Yingmei; Zhao, Haidan; Tao, Jie

DOI
10.1016/j.compstruct.2020.112858

Publication date
2020

Document Version
Accepted author manuscript

Published in
Composite Structures

Citation (APA)
Li, H., Wang, H., Alderliesten, R., Xiang, J., Lin, Y., Xu, Y., Zhao, H., & Tao, J. (2020). The residual stress characteristics and mechanical behavior of shot peened fiber metal laminates based on the aluminium-lithium alloy. *Composite Structures*, *254*, Article 112858. https://doi.org/10.1016/j.compstruct.2020.112858

The Residual Stress Characteristics and Mechanical Behavior of Shot Peened Fiber Metal Laminates based on the Aluminum-lithium Alloy

Huaguan Li[1, 3*], Hao Wang[2], René Alderliesten[3], Junxian Xiang[2], Yanyan Lin[2], Yingmei Xu[2], Haidan Zhao[1], Jie Tao [2*]

[1] Jiangsu Key Laboratory of Advanced Structural Materials and Application Technology, Nanjing Institute of Technology, Nanjing 211167, China

[2] College of Material Science and Technology, Nanjing University of Aeronautics and Astronautics, Nanjing 210016, China

[3] Structural Integrity & Composites Group, Faculty of Aerospace Engineering, Delft University of Technology, Delft 2600 GB, The Netherlands

DOI: 10.1016/j.compstruct.2020.112858

Abstract

The effect of shot peen forming on the mechanical behavior of fiber metal laminates (FMLs) based on aluminum-lithium alloy was investigated to reveal the strengthening mechanism and to dispel the suspicion that shot peen forming may result in the performance deterioration of FMLs. The interlaminar, static strength and fatigue properties of shot peened FMLs were investigated. The residual stress characteristics of the shot peened FMLs was also involved with finite element analysis to help understanding the unique mechanical behavior. The results indicated that shot peening caused non-negligible work hardening in external metal layers, which increased the tensile strength of the laminates. But the work hardening did not deteriorate the elongations of FMLs since the failure still

* Corresponding author. Tel.: +86-25-5211-2911
E-mail addresses: lihuaguan@nuaa.edu.cn (Huaguan Li).
* Corresponding author. Tel.: +86-25-5211-2911
E-mail addresses: taojie@nuaa.edu.cn (Jie TAO).

dominated by the limitation of fiber failure strain. Moreover, two yield stages were observed in the tensile tests of shot peened FMLs owing to the great difference in stress states between external and internal metal layers. The compressive stress introduced by shot peening effectively improved the FCG properties of FMLs. All metal layers possessed similar crack propagation rates despite that the stress difference was up to 300MPa, which indicated that the fiber bridging effect still dominated the FCG of FMLs.

Keywords: Fiber metal laminates; Aluminum-lithium alloy; Shot peen forming; Mechanical behavior; Residual stress

Nomenclature

p positive pressure

q Mises equivalent stress

ω_{D} state variables related to plastic deformation

$\bar{\varepsilon}^{pl}$ equivalent plastic strain

$\varepsilon^{f,T}$ failure strain of tension

$\varepsilon^{f,C}$ failure strain of compression

G fracture toughness

d damage variable

L_c characteristic length

ε^{f} maximum strain

t thickness of the cohesive element

η mixed failure index

1 Introduction

Fiber Metal Laminates (FMLs) possess excellent fatigue and impact resistance[1, 2], which are still attractive in aviation and high-speed train. The well-known GLARE laminates usually choose 2024-T3 aluminum alloy as the metal layer and S-glass fiber composites as the fiber layer [3, 4]. Except outstanding impact and fatigue, it also exhibits good residual and blunt notch strength. Also, GLARE always possesses stable crack propagation behavior after suffering serious irreversible damage [5, 6]. Though carbon fiber composites are getting more attention, GLARE is still an important material in the field of aviation, rail transit, and other lightweight components that both require impact resistance and fatigue. Besides, GLARE has the potential to further improve the overall performance. Considering the lower costs and better damage tolerance, third generation aluminum-lithium alloy [7, 8], replace 2024-T3 aluminum alloy, is one of the desired choose to develop novel FMLs [9-11].

FML components are usually manufactured referring conventional forming method of metal panels. However, limited failure strain of the glass fiber increase forming difficulties, which is one of the biggest factors limiting the application of FMLs [12, 13]. Recent years, the shot peen forming [14, 15] has been developed for FMLs. It provides effective as well as economical solution for the manufacturing of complex FML components. Moreover, the residual stress field introduced by shot peening also beneficial to the fatigue properties. Lots of investigations have focused on the conventional shot peening or laser forming of FMLs. The unique failure behavior and deformation rules, comparing with metal panels, are revealed [16, 17]. Meanwhile, the suitable balls and shot peen

parameters are obtained for both conventional shot peening or laser forming [18-20]. In view of the essential problem of "stress dominant deformation" in shot peen forming, our previous research also focused on the residual stress evolution of FMLs during the shot peen forming. The relationship between processes, residual stress distribution and forming curvature is finally established [21]. However, studies have never addressed on the mechanical behavior variation of FMLs caused by shot peening.

FMLs has more complex mechanical behavior than conventional aluminum alloy owing to the laminating structure and large difference in mechanical response of each component. Firstly, the single metal layer of FMLs or conventional GLARE is 0.3-0.5 mm, which means that the local plastic deformation caused by shot peening occupies a large proportion through that thickness. The serious work-hardening and embrittlement of shot peened metal layers may promote the formation and propagation of cracks. Meanwhile, the depth of the pit is non-ignorable as the single metal layer is extremely thin. Every pit may act as the apparent defect, inducing fracture during the loading. Moreover, the previous work indicated that large size balls or high shot peen intensity could results in the delamination of metal/fiber interfaces. Even the optimized forming parameters did not cause obvious defects in FMLs, the interlaminar properties of shot peened laminates should be verified. Besides, the complicated residual stress characteristics greatly affect the mechanical behavior of FMLs. For conventional aluminum-lithium panels, the shot peened surface with a certain depth possesses obvious compressive stress while most other areas present tensile stress. The change in stress is continuous and gradual along the thickness. However, non-negligible residual stress field has already formed in FMLs during the curing process owing to different thermal expansion coefficient of each component [22]. The metal layers usually possesse a tensile stress of 40-45MPa while the

fiber layers exhibit a compressive stress of 65-70MPa. Then, shot peening introduces significant compressive stress in the external aluminum-lithium layers, which results in a stress rebalance within the whole laminate. residual stress change discontinuously on the fiber/metal and 0°fiber/90°fiber interface due to the different modulus of each component.

Hence, our research primarily tried to investigate the properties variation of FMLs after shot peening through evaluating the interlaminar properties, tensile properties and fatigue crack growth. This work revealed the strengthening mechanism of shot peening on FMLs, and by doing so further demonstrated the feasibility of shot peen forming.

2 Experimental

2.1 Manufacturing of FMLs

The 2060 Al-Cu-Li alloy with the initial thickness of 0.3mm mm was used as the metal layer [9], while S4-glass/epoxy prepregs used as the fiber layer. Firstly, all the metal layers with double face were anodized using phosphoric acid to build a rough surface structure. Secondly, J116 structural adhesive was also adopted to further enhance the bonding between fiber and metal layers. Thirdly, an FML with a 3/2 lay-up were fabricated (i.e. cross-ply, see Fig.1). The curing process was conducted in an autoclave, and the curing process is shown in Fig. 2.

2.2 Shot peen forming of FMLs

FMLs were shot peened in the production line of AVIC Xi'an Aircraft Industry (group) Co., Ltd (see Fig. 3(a)), since the motivation of this work was to verify whether shot peen forming could be used in the real manufacturing of actual FMLs components. Differ from conventional metal panels, FMLs were shot peened using AZB425 ceramics balls instead of cast steel balls to achieve a good surface quality and avoid possible failure behavior [18]. Double faced shot peening was adopted to

prepare flat specimen instead of curved, see Fig. 3(b). The bottom surface of FMLs was bonded to the mold and the upper metal surface was shot peened. Then, the specimens were flipped 180° and the above operation was repeated. Before shot peening, the FMLs were machined to required sizes using CNC milling. Then, the A and B processes were adopted, as the detail parameters shown in Table 1. Two shot peening intensities were selected.

2.3 Characterization and testing of FMLs

The floating roller peel test of FMLs was carried out to evaluate the interlaminar properties of shot peened FMLs, see Fig. 4(a). a peeling speed of 100 mm/min was applied based on ASTM D3167-2003. Meanwhile, the statics properties of FMLs were studied through tensile test with reference of ASTM D3039, see Fig. 4(b). A test loading speed of 2 mm/min was used and the deformation was measured by laser extensometer. values for peeling and tensile properties were obtained as an average of five samples.

Fatigue crack growth (FCG) tests was conducted in an MTS 370 to better reveal the effect of shot peening (see Fig. 5), especially the change in residual stress, on the fatigue properties of FMLs. Center crack tension specimens was used according to ASTM 647. The precrack with the length of 1mm was prepared. The crack propagated under the constant cyclic stress (S_{max}=120MPa, R=0.1), and was recorded using a digital camera system.

2.4 Finite element model establishment

The residual stress of as-manufactured as well as shot peened FMLs was analyzed using FE model. The simulation FE software, ABAQUS/Standard 6.14, was used to establish a three-dimensional finite element model. Each layer was individually meshed to appraise stress variation situation of laminates. Figure 6 illustrates the discrete model of shot peened sample and the boundary

condition. The residual stress generated during the curing process was obtained through the thermoelastic finite element model [23]. The compressive stress in shot peened surface introduced by shot peening was calculated according to the investigations on Quasi-static indentation of FMLs [24], which was then defined in the cured FMLs model.

The Aluminum-Lithium alloy layers were simulated using an isotropic elastoplastic model and the C3D8R elements were chosen to mesh. Strain-strengthening behavior was defined by measured stress-strain curve data. Initial damage was judged with ductile damage criterion which was described as the following equation[21].

$$\omega_D = \int \frac{d\bar{\varepsilon}^{pl}}{\bar{\varepsilon}_D^{pl}(\eta, \dot{\bar{\varepsilon}}^{pl})} \tag{1}$$

The damage evolution is shown as the following equations.

$$D^{el} = (1-d)D_0^{el} \tag{2}$$

$$\sigma = D^{el}:(\varepsilon - \bar{\varepsilon}^{pl}) \tag{3}$$

The parameters of basic mechanical property of aluminum-lithium were listed in Table 2**.**

Fiber layers were defined as orthotropic linear elastic material, which were also modelled by C3D8R elements. A progressive damage criterion was applied for the damage initiation criterion and damage was judged according to the following equation[25].

$$f_f = \sqrt{\frac{\varepsilon_{11}^{f,\mathrm{T}}}{\varepsilon_{11}^{f,\mathrm{C}}}(\varepsilon_{11})^2 + \left[\varepsilon_{11}^{f,\mathrm{T}} - \frac{\left(\varepsilon_{11}^{f,\mathrm{T}}\right)^2}{\varepsilon_{11}^{f,\mathrm{C}}}\right]\varepsilon_{11}} > \varepsilon_{11}^{f,\mathrm{T}} \tag{4}$$

$$f_m = \sqrt{\frac{\varepsilon_{22}^{f,T}}{\varepsilon_{22}^{f,C}}(\varepsilon_{22})^2 + \left[\varepsilon_{22}^{f,T} - \frac{\left(\varepsilon_{22}^{f,T}\right)^2}{\varepsilon_{22}^{f,C}}\right]\varepsilon_{22} + \left(\frac{\varepsilon_{22}^{f,T}}{\varepsilon_{22}^{f}}\right)^2 (\varepsilon_{12})^2} > \varepsilon_{22}^{f,T} \tag{5}$$

The damage evolution law was defined by equations (6) and (7).

$$d_f = 1 - \frac{\varepsilon_{11}^{f,T}}{f_f} e^{\left[-C_{11}\varepsilon_{11}^{f\cdot T}(f_f - \varepsilon_{11}^{f\cdot T})L^C/G_f\right]} \tag{6}$$

$$d_m = 1 - \frac{\varepsilon_{22}^{f,T}}{f_m} e^{\left[-C_{22}\varepsilon_{22}^{f\cdot T}(f_m - \varepsilon_{22}^{f\cdot T})L^C/G_m\right]} \tag{7}$$

Besides, interface interaction was defined by cohesive model, which was an interface unit without thickness. The constitutive relation of the model was the traction separation mode of stress and strain. Quads damage criterion was used to judge the damage initiation and B-K law was selected to predict the delamination damage respectively described in Eq. (8) and Eq. (9).

$$\left(\frac{\varepsilon_n}{\varepsilon_n^f}\right)^2 + \left(\frac{\varepsilon_s}{\varepsilon_s^f}\right)^2 + \left(\frac{\varepsilon_t}{\varepsilon_t^f}\right)^2 = 1 \quad (8)$$

$$G_{IC} + \left(G_{//C} - G_{IC}\right)\left(\frac{G_{//C}}{G_T}\right)^{\eta} = G_C \quad (9)$$

The corresponding mechanical properties of the fiber layer and cohesive layer were taken from our previous research [25].

3 Results and discussion

3.1 Interlaminar properties

The SEM morphology of shot peened FMLs was shown in Fig. 7. The roughness surface caused by local plastic deformation is observed. Meanwhile, the indentation depth was about 20-30% of the 0.3 mm thin metal layer. All the fiber layers remained intact.

The shot peened FMLs exhibit similar peeling strength on the shot peened metal/fiber surface comparing with the as-manufactured samples, as shown in Table 3. The shear stress in fiber/metal interface is also analyzed. Similar to as-manufactured FMLs, the laminates after shot peening exhibit no obvious interfacial shear stress in most areas, see Fig. 8. However, the shear stress around the edges, caused by free boundary effect, increases from 7.85MPa to 15.69MPa after shot peening (taking process B as an example). The FMLs exhibit an interlaminar shear stress of 55MPa, which is much larger than the shear stress generated at the edges. Even so, suitable shot peening process should be carefully selected. Higher shot peening intensity undoubtedly results to larger interlaminar shear stress around edge, further increase the risk in delamination of the laminates. The results above well

explain the failure behavior in our previous research that the excessive shot peening intensity always cause the delamination from the edge [18].

The above results suggest that the applied shot peening processes have no obvious effect to the interlaminar properties of the FMLs. The consistent peeling strength makes it easier to compare the other mechanical properties before and after shot peening, since the interlaminar bonding strength may affect the performance (e.g. FCG) of FMLs.

3.2 Tensile properties of FMLs

For the tensile load-displacement curves indicated in Fig. 9, All the curves go smoothly without any inflection point, which indicates that the shot peened samples possess no abnormal fracture or damage.

The yield behavior is further analyzed in the amplified stress-strain curves, based on the selected area, see Fig. 10. The as-manufactured FMLs maintain a good bilinear relationship while the shot peened laminates present two yield stages. The residual stress characteristics of the whole laminates are provided to help explain the above phenomenon, as shown in Fig. 11. Considering the different thermal expansion coefficient between fiber and metal layers, the three aluminum-lithium layers exhibit similar tensile stress before shot peening. Hence, the aluminum-lithium layers yield at the same stress level, presenting the yield stress of 265.72MPa. However, shot peening introduces significant compressive stress in the external aluminum-lithium layers, which results in a stress rebalance within the whole laminate. The internal aluminum-lithium layer exhibits greater tensile stress in excess of 200 MPa. The obvious difference in stress state of external and internal metal layers leads to two yield point at 249.72MPa and 325.89MPa respectively.

Meanwhile, Fig. 9 also indicates that the failure strain of the laminate before and after shot

peening has no obvious change. Usually, FMLs or conventional GLARE fail mainly by the limitation of fiber failure strain. Comparing to the significant stress changes in metal layers, the stress variation in fiber layers, relative to their ultimate strength, hardly affects the initial strain. Hence, the effect of shot peening on elongation of FMLs at break is quite small.

Also, the shot peening increases the tensile strength of FMLs, see Fig. 12. Usually, the residual stress variation in the laminates hardly changes the ultimate strength. Therefore, the possible reason may owe to the work hardening of shot peened metal layers. The microhardness results shown in Table 4 prove our speculation. The obvious work hardening exists in shot peened metal layers.

Work hardening always leads to a decreased plasticity and toughness of aluminum panels. However, the work hardening of external metal layers hardly affects the elongation of FMLs since the failure mainly dominates by the limitation of fiber failure strain.

3.3 Fatigue crack growth

Shot peening leads to the increase of roughness and work hardening of the aluminum-lithium layer, which may deteriorate the fatigue properties of FMLs. However, shot peening also results in the significant change in residual stress field of FMLs. Especially the positive compressive stress in the surface metal layers is beneficial to prevent the generation as well as propagation of cracks.

The shot peened FMLs exhibit more desired FCG properties, as presented in Fig. 13. Almost twice the number of cycles is required for the laminates shot peened by process B comparing with the as-manufactured one.

Actually, the typical failure of FMLs in FCG tests includes crack growth in the aluminum-lithium layers and delamination at the metal/prepregs interfaces, which owes to the fiber bridging effect [26-28]. The failure behavior at the metal/fiber interfaces also influences the FCG properties.

Though the fibers remain intact in all the specimens, as presented in Fig. 14, smaller delamination is observed in FMLs after shot peening. The delamination shape, together with the obtained results in Fig. 11, prove that the shot peening significantly improves the FCG properties of FMLs.

Without doubt the introduced compressive stress in external metal layers effectively reduces the rate of crack propagation. However, according to the residual restress analysis in Fig. 11, the internal metal layer exhibits a large tensile stress of more than 200 MPa. Based on the internal stress distribution, one could speculate that the internal metal layer, compared to the external ones, exhibits quite different FCG, i.e. it may propagate faster. Hence, two sets of FCG tests have been conducted to study this hypothesis. The FCG tests were terminated during the experiments and the other fiber and metal layers were removed to observe the crack length in the internal metal layer. The external metal layers are easily etched by sodium hydroxide solution while fiber layers were removed mechanically after heated to 400℃. Two sets of FCG tests were stopped when the crack reached about 13.3mm and 26.6mm to compare the actual crack length in internal and external layers.

The interesting results shown in Fig. 15 indicates that instead of the expected different crack growth rates, the three metal layers have similar crack growth rates. Two factors together determine the crack propagation rate of the metal layers. One is metal layers' own stress state while the other is the bridging effect of fiber layers. The advantage of internal metal layers is the double faced bridging by fiber layers. Usually, the fiber bridging effect greatly improve the fatigue properties in as-manufactured FMLs[29, 30]. The results above indicate that fiber bridging effect still dominates the FCG FMLs after shot peening despite that the stress difference in metal layers themselves is up to 300MPa.

The crack length is also analyzed based on "compliance method"[31]. FMLs possess more

complicated FCG mechanism than conventional metal materials. The crack length, in general, is recorded using a digital camera system instead of deflection method to ensure the accuracy. But the deflection method is quicker on the data acquisition. Figure 16 is the Tpartially enlarged view of a-N curve obtained by deflection method (Data collection was accelerated to 1 per second). Smooth a-N curve is obtained for as-manufactured laminates but jagged curve is found for shot peened specimen. The crack growth behavior is always dominated by the stress intensity factor around crack tip. From the view point of a single shot impact, non-homogeneous stress state as well as geometry exist around the crater, which results in the constantly changing of stress intensity factor. The fluctuating stress intensity factor over a limited range appears as the jagged lines in a-N curve.

4. Conclusions

The shot peening introduced significant compressive stresses in the external aluminum-lithium layers, which led to the stress rebalance of FMLs. As a result, great difference in stress states between external and internal metal layers was generated. The stress rebalance during shot peening hardly resulted in the great variation of interlaminar shear stress in the most area of metal/fiber interface. However, the shear stress around the edges, caused by free boundary effect, increased obviously after shot peening. It was the reason that excessive shot peening intensity always caused the delamination from the edge. Applied with suitable shot peening process (process A and B), FMLs was found no obvious damage or delamination and exhibit consistent peeling strength comparing with the as-manufactured lamiantes. Shot peening caused non-negligible work hardening in external metal layers, which increased the tensile strength of the whole laminates. But the work hardening did not deteriorate the elongations of FMLs since the failure was mainly dominated by the limitation of fiber failure strain. Moreover, two yield stages were found in the tensile tests of shot peened FMLs owing

to the great difference in stress states between external and middle metal layers. The compressive stress introduced by shot peening great improved the FCG properties of FMLs. Meanwhile, the fiber bridging effect still dominated the fatigue properties of FMLs. Tough the internal metal layer exhibited the tensile stress in excess of 200 MPa, it still possessed similar crack propagation rate comparing with the external ones, which mainly owed to the double faced bridging effect.

Acknowledgements

The authors gratefully acknowledge the financial support of the National Natural Science Foundation of China (51705235), the Natural Science Foundation of Jiangsu Province (BK20170762), Jiangsu Jiangsu key R & D plan (BE2018125), Opening Project of Jiangsu Key Laboratory of Advanced Structural Materials and Application Technology (ASMA201803), Qing Lan Project.

References

[1] Chai G B, Manikandan P. Low velocity impact response of fibre-metal laminates–A review. Compos Struct 2014; 107: 363-381.

[2] Şen I, Alderliesten R C, Benedictus R. Lay-up optimisation of fibre metal laminates based on fatigue crack propagation and residual strength. Compos Struct 2015; 124: 77-87.

[3] Morinière F D, Alderliesten R C, Sadighi M, et al. An integrated study on the low-velocity impact response of the GLARE fibre-metal laminate. Compos Struct 2013; 100: 89-103.

[4] Young J B, Landry J G N, Cavoulacos V N. Crack growth and residual strength characteristics of two grades of glass-reinforced aluminium 'Glare'. Compos Struct 1994, 27(4): 457-469.

[5] Alderliesten RC, Homan JJ. Fatigue and damage tolerance issues of GLARE in aircraft structures. Int J Fatigue 2006; 28(10): 1116-23.

[6] Wu G, Yang JM. The mechanical behavior of GLARE laminates for aircraft structures. Jom 2005;57(1):72-79.

[7] Lavernia E J, Srivatsan T S, Mohamed F A. Strength, deformation, fracture behaviour and ductility of aluminium-lithium alloys. J Mater Sci 1990; 25(2): 1137-1158.

[8] El-Aty A A, Xu Y, Guo X, et al. Strengthening mechanisms, deformation behavior, and anisotropic mechanical properties of Al-Li alloys: A review. J Adv Res 2018; 10: 49-67.

[9] Li H, Hu Y, Xu Y, et al. Reinforcement effects of aluminum-lithium alloy on the mechanical properties of novel fiber metal laminate. Compos Part B 2015; 82: 72-7.

[10] Li H, Hu Y, Liu C, et al. The effect of thermal fatigue on the mechanical properties of the novel fiber metal laminates based on aluminum-lithium alloy. Compos Part A 2016; 84: 36-42.

[11] Alderliesten R C, Rans C D, Beumler T, et al. Recent Advancements in Thin-Walled Hybrid Structural Technologies for Damage Tolerant Aircraft Fuselage Applications[M]//ICAF 2011 Structural Integrity: Influence of Efficiency and Green Imperatives. Springer, Dordrecht, 2011: 105-117.

[12] Gresham J, Cantwell W, Cardew-Hall M J, et al. Drawing behaviour of metal-composite sandwich structures. Compos Struct 2006; 75(1): 305-12.

[13] Mosse L, Compston P, Cantwell W J, et al. The development of a finite element model for simulating the stamp forming of fibre-metal laminates. Compos struct 2006; 75(1): 298-304.

[14] Hu Y, Zheng X, Wang D, et al. Application of laser peen forming to bend fibre metal laminates by high dynamic loading. J Mater Process Tech 2015; 226: 32-39.

[15] Hu Y, Zhang W, Jiang W, et al. Effects of exposure time and intensity on the shot peen forming characteristics of Ti/CFRP laminates. Compos Part A 2016; 91: 96-104.

[16] Russig C, Bambach M, Hirt G, et al. Shot peen forming of fiber metal laminates on the example of GLARE®. Int J Mater Form, 2014, 7(4): 425-438.

[17] Li H, Lu Y, Han Z, et al. The shot peen forming of fiber metal laminates based on the aluminum-lithium alloy: Deformation characteristics. Compos Part B 2019; 158, 279-285.

[18] Li H, Zhang W, Jiang W, et al. The feasibility research on shot-peen forming of the novel fiber metal laminates based on aluminum-lithium alloy. Int J Adv Manuf Tech 2018; 96(1-4): 587-596.

[19] Gisario A, Barletta M. Laser forming of glass laminate aluminium reinforced epoxy (GLARE): On the role of mechanical, physical and chemical interactions in the multi-layers material. Opt Laser Eng 2018; 110: 364-376.

[20] Carey C, Cantwell W J, Dearden G, et al. Towards a rapid, non-contact shaping method for fibre metal laminates using a laser source. Int J Adv Manuf Tech 2010; 47(5-8): 557-565.

[21] Li H, Lu Y, Xiang J, et al. Residual Stresses and Failure Behavior of GFRP/Al-Li Laminates after Single and Multiple Shot's Indentation under Quasi-static. Compos Part A 2020; 130: 105761.

[22] Abouhamzeh M, Sinke J, Jansen K M B, et al. Closed form expression for residual stresses and warpage during cure of composite laminates. Compos Struct 2015, 133: 902-910.

[23] Xu Y, Li H, Yang Y, et al. Determination of residual stresses in Ti/CFRP laminates after preparation using multiple methods. Compos Struct 2019; 210: 715-723.

[24] Du D, Hu Y, Li H, et al. Open-hole tensile progressive damage and failure prediction of carbon fiber-reinforced PEEK-titanium laminates. Compos Part B 2016; 91:65-74.

[25] Hua X, Li H, Lu Y, et al. Interlaminar fracture toughness of GLARE laminates based on asymmetric double cantilever beam (ADCB). Compos Part B 2019; 163:175-184.

[26] Alderliesten R C, Homan J J. Fatigue and damage tolerance issues of Glare in aircraft structures. Int J Fatigue 2006; 28(10): 1116-1123.

[27] Alderliesten R C. Fatigue and fracture of fibre metal laminates[M]. New York, USA: Springer, 2017.

[28] Wang W, Rans C, Zhang Z, et al. Prediction methodology for fatigue crack growth behaviour in Fibre Metal Laminates subjected to tension and pin loading. Compos Struct 2017, 182: 176-182.

[29] Langdon GS, Cantwell WJ, Nurick GN. Localised blast loading of fibre-metal laminates with a polyamide matrix. Compos Part B 2007; 38(7): 902-13.

[30] Chang P Y, Yang J M. Modeling of fatigue crack growth in notched fiber metal laminates. Int J Fatigue 2008; 30(12): 2165-74.

[31] Alderliesten R C. Fatigue crack propagation and delamination growth in Glare, PhD Thesis, Delft University of Technology, 2005.

Table 1 Parameters of FMLs shot peening process

Process	Ball type	Intensity	Coverage (%)	Shot peening time (s)
A	AZB425	0.097A	100	5
B	AZB425	0.155A	100	5

Table 2 Mechanical properties of aluminum–lithium layer

Material	Young's modulus/GPa	Poisson's ratio	Yield strength/MPa	Tensile strength/MPa
aluminum–lithium	82.50	0.33	379.86	479.12

Table 3 Effect of shot peening on the peeling strength of FMLs

Shot peening process	Average peeling strength (N/mm)
As-manufactured	4.51±0.21
Process A, double-faced	4.46±0.30
Process B, double-faced	4.62±0.28

Table 4 Effect of shot peening on the microhardness of the surface of Al-Li alloy layer

Shot peening process	Microhardness (HV0.2)
As-manufactured	114.70±2.65
Process A	138.25±3.50
Process B	149.73±3.38

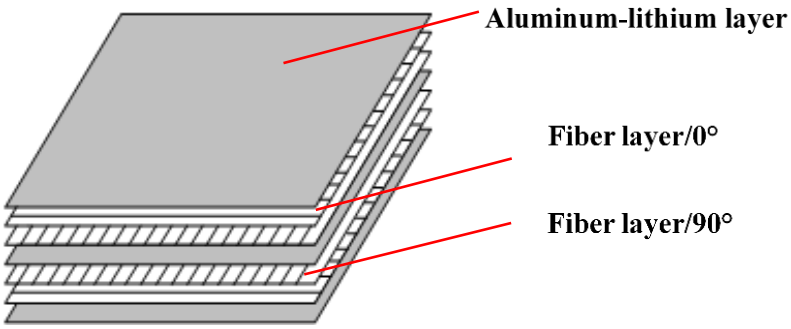

Fig. 1 The FMLs studied constitute an FML3-3/2-0.3 lay-up

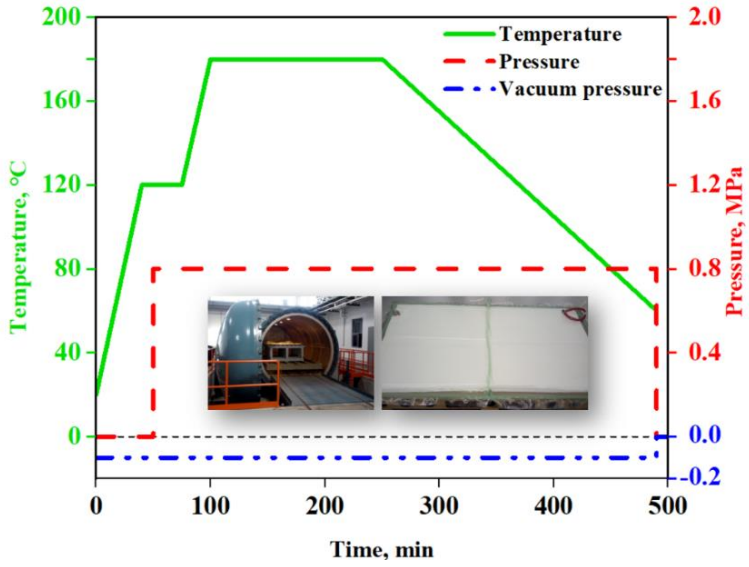

Fig. 2 The curing process of the FMLs in autoclave

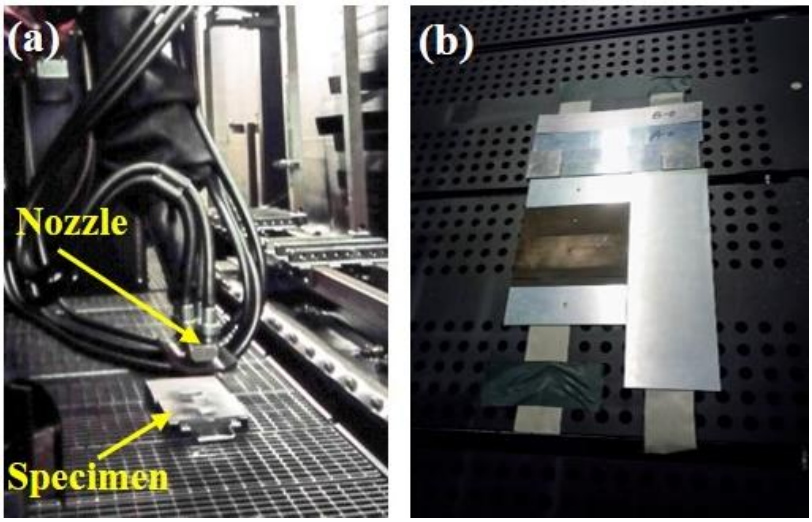

Fig. 3 The shot peen forming process of FMLs: (a) the objective graph; (b) specimens to be processed

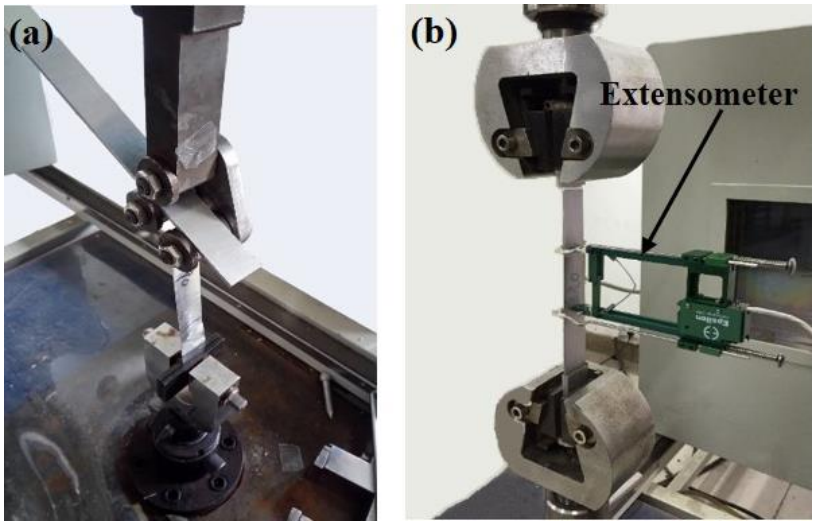

Fig. 4 The objective graph of the mechanical tests: (a) floating roller peel test;(b) tensile test

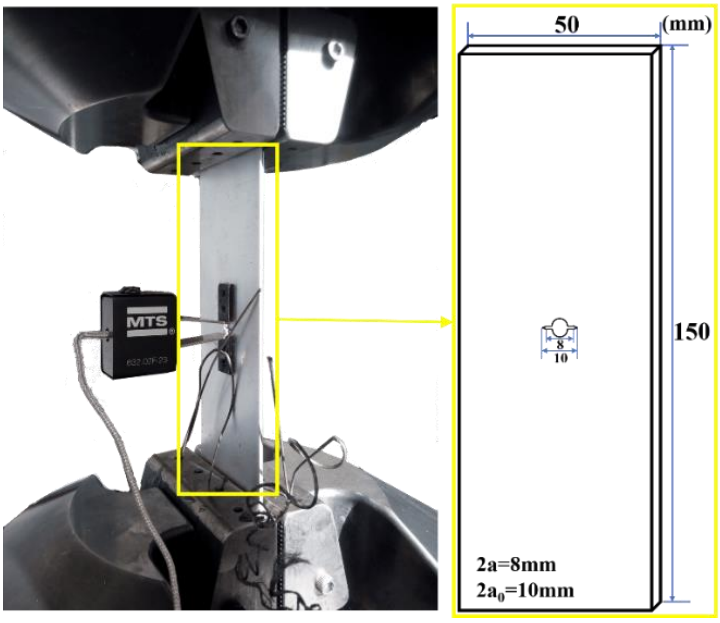

Fig. 5 The FCG test of FMLs

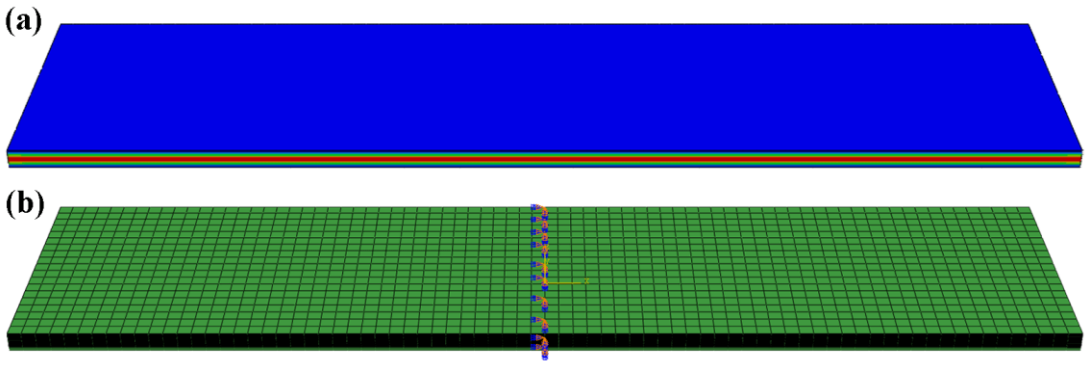

Fig. 6 Images of the model: (a) meshing of the FMLs; (b) boundary conditions

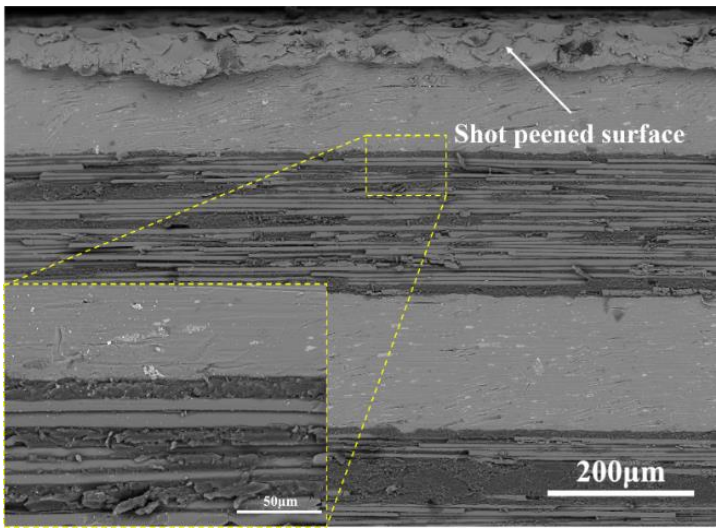

Fig. 7 The SEM morphology of shot peened FMLs

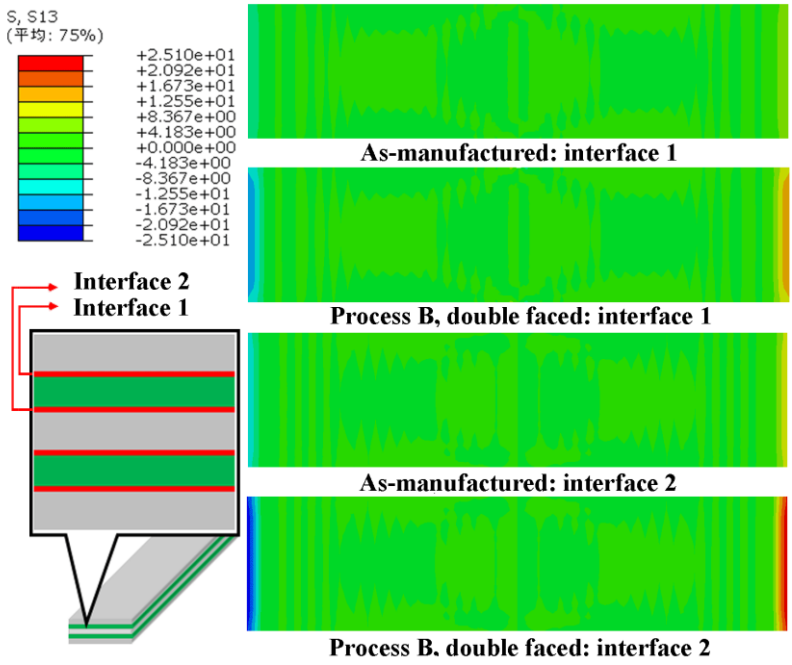

Fig. 8 interfacial shear stress of FMLs before and after shot peening

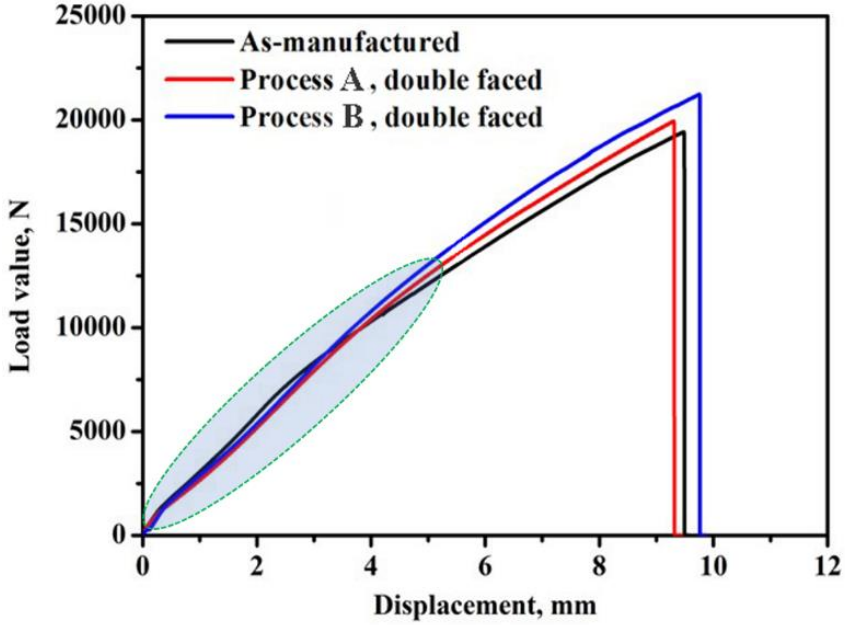

Fig. 9 Tensile load-displacement curves of FMLs before and after shot peening

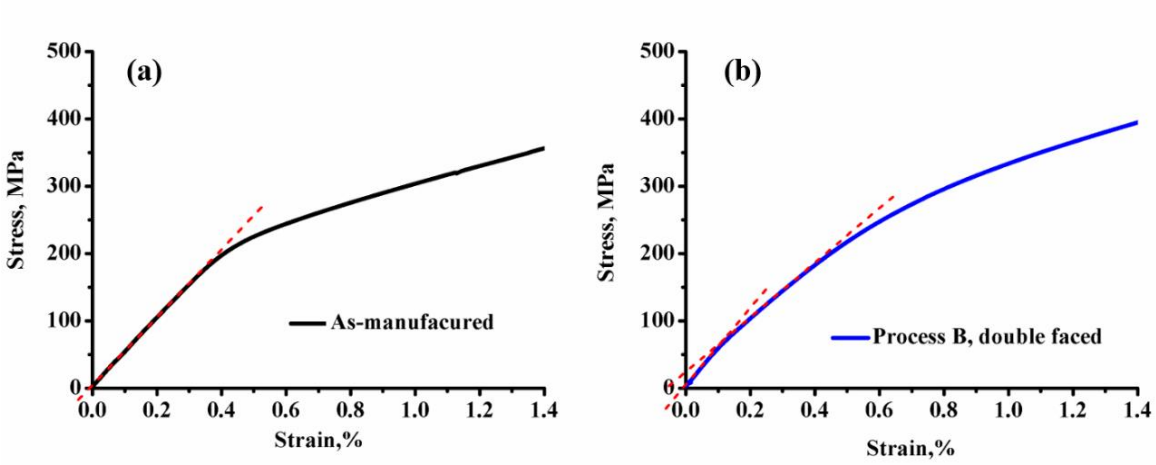

Fig. 10 Stress-strain curves of FMLs: (a) as-manufacured; (b) process B, double faced

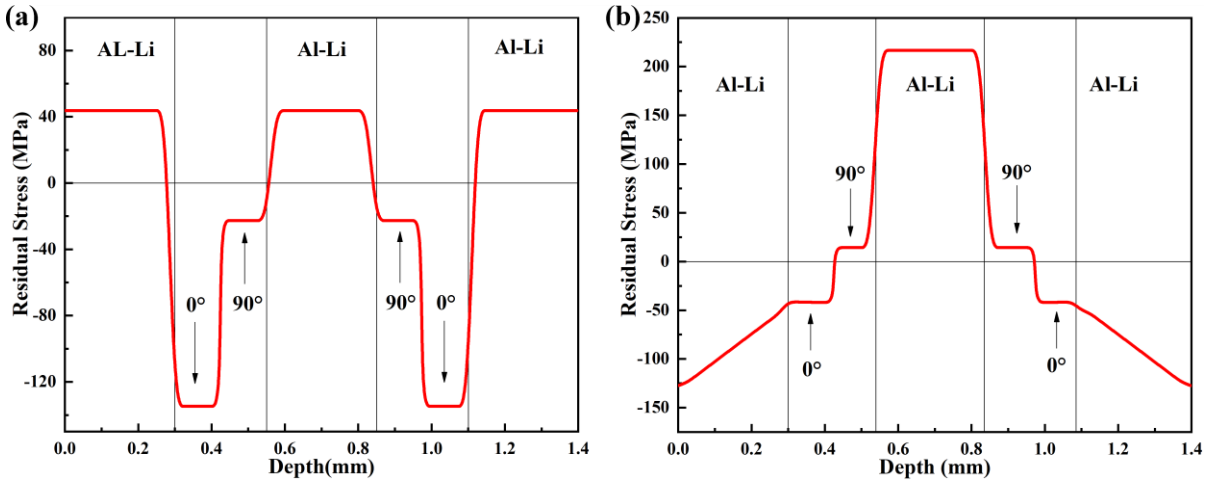

Fig. 11 The residual stress distribution in FMLs: (a) as-manufactured (b) process B, double faced

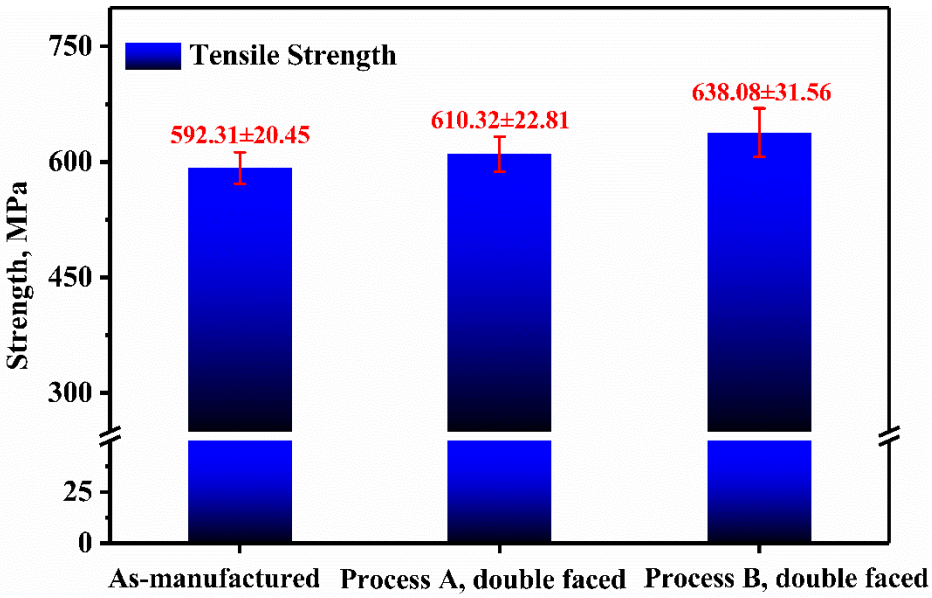

Fig. 12 Effect of shot peening on tensile properties of FMLs

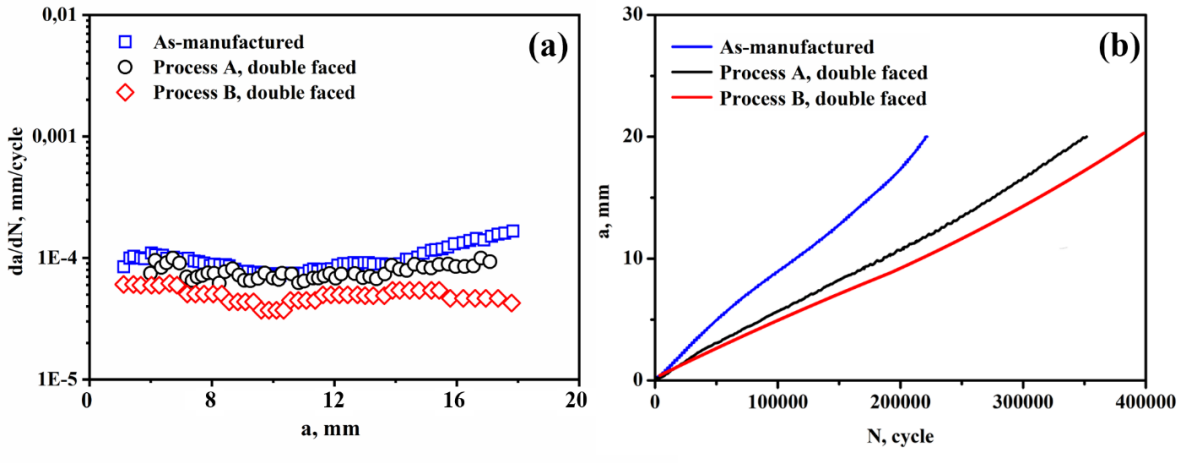

Fig. 13 Effect of shot peening on fatigue crack growth rate of FMLs: (a) da/dN-a curve; (b) a-N curve

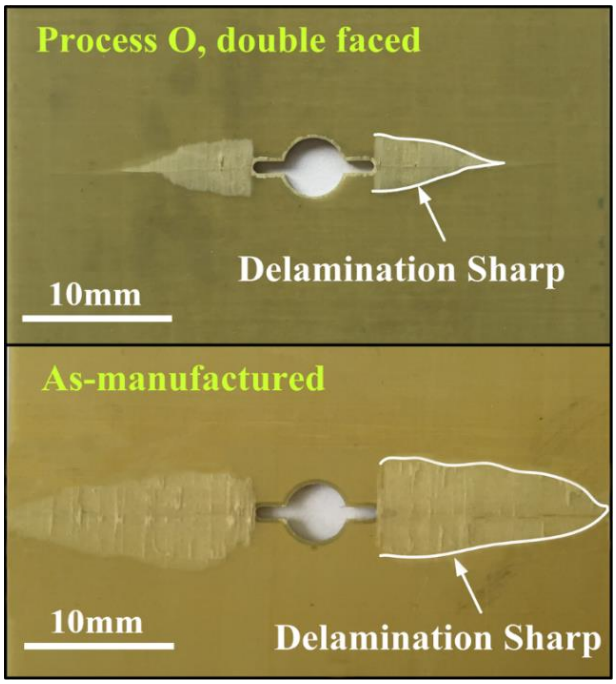

Fig. 14 Damage morphology of FMLs fiber layer before and after shot peening

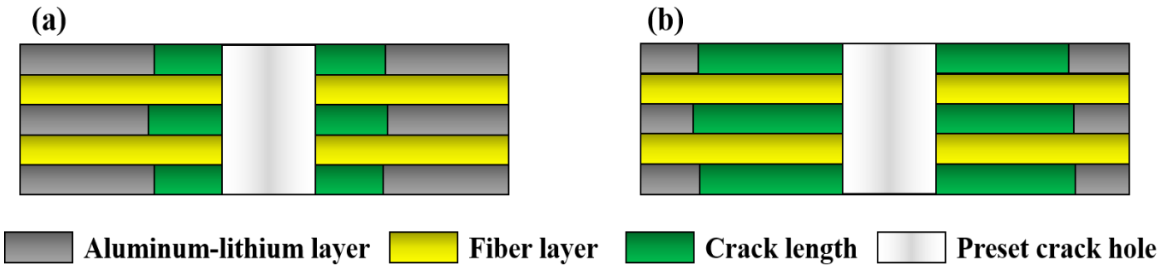

Fig. 15 crack length in internal and external layers of FMLs shot peened by process B:

(a) crack reached about 13.3mm; crack reached about 26.6mm

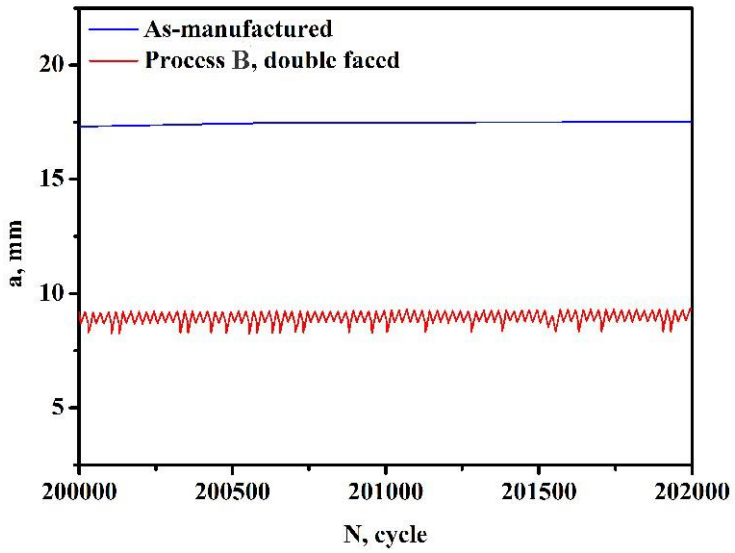

Fig. 16 Jagged a-N curve of shot peened FMLs